HHS Public Access

Author manuscript

Cancer Cell. Author manuscript; available in PMC 2017 May 09.

Published in final edited form as:

Cancer Cell. 2016 May 9; 29(5): 639–652. doi:10.1016/j.ccell.2016.03.026.

Tight Junction Protein 1 Modulates Proteasome Capacity and Proteasome Inhibitor Sensitivity in Multiple Myeloma via EGFR/JAK1/STAT3 Signaling

Xing-Ding Zhang[1,2,3], **Veerabhadran Baladandayuthapani**[4], **Heather Lin**[4], **George Mulligan**[5], **Bin Li**[5], **Dixie-Lee W. Esseltine**[5], **Lin Qi**[3], **Jianliang Xu**[6], **Walter Hunziker**[6], **Bart Barlogie**[7], **Saad Z. Usmani**[7,8], **Qing Zhang**[7,8], **John Crowley**[9], **Antje Hoering**[9], **Jatin J. Shah**[1], **Donna M. Weber**[1], **Elisabet E. Manasanch**[1], **Sheeba K. Thomas**[1], **Bing-Zong Li**[1], **Hui-Han Wang**[1], **Jiexin Zhang**[4], **Isere Kuiatse**[1], **Jin-Le Tang**[2], **Hua Wang**[1], **He Jin**[1], **Jing Yang**[1], **Enrico Milan**[10], **Simone Cenci**[10], **Wen-Cai Ma**[1], **Zhi-Qiang Wang**[1], **Richard Eric Davis**[1,12], **Lin Yang**[2,3,*,12], and **Robert Z. Orlowski**[1,11,*,12]

[1]Department of Lymphoma/Myeloma, The University of Texas MD Anderson Cancer Center, Houston, TX 77030, USA

[2]Cyrus Tang Hematology Center, Soochow University, Suzhou, Jiangsu 215123, China

[3]Xi'an Jiaotong University Suzhou Academy, Suzhou, Jiangsu 215123, China

[4]Department of BioSTATistics, The University of Texas MD Anderson Cancer Center, Houston, TX 77030, USA

[5]Millennium: The Takeda Oncology Company, Cambridge, MA 02139, USA

[6]Institute of Molecular and Cell Biology, Singapore 138673, Republic of Singapore

[7]Myeloma Institute for Research and Therapy, University of Arkansas for Medical Sciences, Little Rock, AR 72205, USA

[8]Department of Hematologic Oncology, Levine Cancer Institute, Carolinas Healthcare System, Charlotte, NC 28204, USA

[9]Cancer Research and BioSTATistics, Seattle, WA 98101, USA

[*]Correspondence: yanglin@suda.edu.cn (L.Y.), rorlowsk@mdanderson.org (R.Z.O.).
[12]Co-senior author

SUPPLEMENTAL INFORMATION

Supplemental Information includes Supplemental Experimental Procedures, eight figures, and eight tables and can be found with this article online at http://dx.doi.org/10.1016/j.ccell.2016.03.026.

AUTHOR CONTRIBUTIONS

X.Z. and L.Y. performed the experiments. L.Q. and J.T. contributed to the protein and cell death measurements, while E.M. and S.C. evaluated proteasome load levels. B.L., I.K., H.J., and J.Y. contributed to the animal studies. V.B., H.L., G.M., B.L., D.W.E., J.Z., B.B., S.Z.U., Q.Z., J.C., and A.H. performed the statistical analyses. R.E.D., W.M., and Z.W. were involved in gene-expression analysis of shRNA cell lines. H.W. was involved in construction of plasmids and lentivirus vectors. X.J. and W.H. developed *Tjp1* knockout murine embryonic stem cells. J.J.S., D.M.W., E.E.M., and S.K.T. provided access to primary samples and helped in analyzing flow data. X.Z., L.Y., and R.Z.O. designed the experiments, and analyzed and interpreted the data. X.Z. and R.Z.O. wrote the manuscript.

An abstract describing some of these data was presented at the 55th Annual Meeting of the American Society of Hematology in New Orleans, LA, in December 2013.

[10]Division of Genetics and Cell Biology, San Raffaele Scientific Institute, Università Vita-Salute San Raffaele, Milan 20132, Italy

[11]Department of Experimental Therapeutics, The University of Texas MD Anderson Cancer Center, Houston, TX 77030, USA

SUMMARY

Proteasome inhibitors have revolutionized outcomes in multiple myeloma, but they are used empirically, and primary and secondary resistance are emerging problems. We have identified TJP1 as a determinant of plasma cell proteasome inhibitor susceptibility. TJP1 suppressed expression of the catalytically active immunoproteasome subunits LMP7 and LMP2, decreased proteasome activity, and enhanced proteasome inhibitor sensitivity in vitro and in vivo. This occurred through TJP1-mediated suppression of EGFR/JAK1/STAT3 signaling, which modulated LMP7 and LMP2 levels. In the clinic, high TJP1 expression in patient myeloma cells was associated with a significantly higher likelihood of responding to bortezomib and a longer response duration, supporting the use of TJP1 as a biomarker to identify patients most likely to benefit from proteasome inhibitors.

INTRODUCTION

Multiple myeloma is a clonal plasma cell disorder and the second most common hematologic malignancy. Patients can develop morbidity due to hypercalcemia, renal insufficiency, anemia, bony lesions, and infections, and these contribute to mortality (Kyle and Rajkumar, 2008). Fortunately, recent advances, including the development of ubiquitin-proteasome pathway (UPP) inhibitors such as bortezomib and carfilzomib, have doubled the median overall survival (OS) of patients. Initially found to be active in refractory disease, later studies led to approvals of bortezomib for relapsed myeloma. Bortezomib-based combinations were then approved for relapsed or refractory and newly diagnosed patients. More recently, carfilzomib, an irreversible proteasome inhibitor (PI), was approved for relapsed/refractory and then relapsed disease, and these agents therefore form an important part of our armamentarium against myeloma.

PIs induce accumulation of ubiquitin-protein conjugates, enhance cellular stress, and trigger apoptosis (Hideshima and Anderson, 2012; Shah and Orlowski, 2009). Plasma cells are uniquely sensitive because the UPP protein turnover capacity is reduced during their differentiation, creating an unfavorable match between proteasome load and capacity (Cenci et al., 2006). Indeed, this balance influences PI sensitivity, with plasma cells having high proteasome capacity showing relative resistance (Bianchi et al., 2009). This was validated by studies showing that acquired bortezomib resistance may emerge in clones that secrete less immunoglobulin. Such cells had lower misfolded protein levels, which reduced plasma cell stress and, thus, reliance on the unfolded protein response (Leung-Hagesteijn et al., 2013). By reducing proteasome load, these cells were PI resistant, raising the possibility that resistance could also be mediated by enhanced proteasomal capacity (Orlowski, 2013).

Despite the demonstrated benefits of PIs, response rates in bortezomib-naive patients in the refractory setting were only 27%, and 43% in the relapsed setting. Similarly, the response

rate to carfilzomib in PI-naive patients was 48% (Hideshima and Anderson, 2012; Shah and Orlowski, 2009), indicating a need for biomarkers to identify patients likely to benefit from PI-based therapy. This could allow triage of patients who are less likely to benefit from PI treatment toward other more effective therapies, thus reducing inconvenience, toxicity, and healthcare costs. Moreover, a biomarker that influenced drug sensitivity could be targeted for chemosensitization, thereby maximizing the benefits of therapy in sensitive patients and providing options to overcome resistance.

RESULTS

TJP1 Is Linked to PI Sensitivity

To identify PI sensitivity biomarkers, we hypothesized that such genes would be differentially expressed in myeloma cells from patients that responded to bortezomib or did not, and in cells that were bortezomib-sensitive or -resistant. We first examined clinically annotated gene-expression datasets from bortezomib clinical trials and, after filtering out probe sets that might be less reliable for biomarker discovery, tested those remaining based on their expression difference in responders and non-responders. The tight junction protein 1 gene (*TJP1*) was ninth on this list using the two-sided t test (Table S1), and fourth using the one-sided t test (not shown). Next, we compared gene expression in bortezomib responders with expression in those who progressed on bortezomib, whereby *TJP1* was ranked eighth in the two-sided and second in the one-sided t test (not shown). To narrow our focus further, we examined gene-expression profiles of ANBL-6 and KAS-6/1 wild-type (WT) and bortezomib-resistant (BR) myeloma cells (Kuhn et al., 2012). Expression of six of these genes was detected above background levels, and *TJP1* was downregulated in BR cells (Figure 1A). In addition, BR RPMI 8226 pooled clones and single-cell subclones expressed lower levels of TJP1 mRNA (Figure 1B) and protein (Figure 1C).

TJP1 plays a role in tight junctions but has not been extensively studied in a myeloma context. Therefore, we selected RPMI 8226 and U266 myeloma cell lines as models that expressed high TJP1 levels, and MOLP-8 as a model that expressed low levels (Figure S1A) to further study the role of TJP1 in myeloma drug resistance. TJP1 knockdown in RPMI 8226 and U266 cells (Figure S1B) with short hairpin RNAs (shRNAs) preserved their viability after bortezomib or carfilzomib exposure, and decreased apoptosis (Figures 1D and 1E). Conversely, TJP1 overexpression (Figure S1C) sensitized MOLP-8 cells to PIs, reducing viability and enhancing apoptosis (Figure 1F). While *NRAS* mutation may reduce bortezomib sensitivity (Mulligan et al., 2014), TJP1 suppression conferred resistance in the presence of WT or mutant *RAS* (Figure 1G).

A recent study reported that PI resistance was mediated by XBP1s^{-} plasma cell precursors de-committed to immunoglobulin synthesis (Leung-Hagesteijn et al., 2013). We therefore examined whether there was any overlap between the XBP1 and TJP1 expression profiles by comparing RPMI 8226/control shRNA cells that express high TJP1 levels with 8226/TJP1 shRNA cells. Gene set enrichment analysis (GSEA) comparing RPMI 8226/control shRNA cells with 8226/TJP1 shRNA cells did not identify the XBP1 signature as being similar to that of TJP1 (Table S2). To test this further we performed cluster analysis, and although there was a correlation between TJP1 and probe set 244377_at for SLC1A4 (Figure S1D),

correlation was lacking with other SLC1A4 probes and other XBP1 targets. Next, we collected 37 XBP1 target gene names from Leung-Hagesteijn et al. (2013), and tested whether each was differentially expressed between bortezomib responders and non-responders. Using a two-sided t test, only four of the genes had a nominal p value <0.05 (Table S3), and only one was predictive of benefit (Figure S1E), while TJP1 was more predictive of both response and duration of benefit.

Impact of TJP1 Is Maintained in the Microenvironment

Proteasome inhibitors are being investigated in other diseases, so we investigated whether TJP1 influenced PI sensitivity in WT murine embryonic stem cells (mESCs) and mESCs in which *Tjp1* had been knocked out (KO) by homologous recombination (Xu et al., 2012). Bortezomib and carfilzomib reduced the viability of WT cells, but the *Tjp1* KO cells were more resistant to both PIs (Figure 2A). Patients with mantle cell lymphoma (MCL) also benefit from bortezomib therapy, and we found that TJP1 knockdown in Mino and JeKo-1 MCL cells conferred relative bortezomib resistance (Figure 2B). Next, we expressed TJP1 in the KO mESCs and RPMI 8226 BR myeloma cells and found that this enhanced their sensitivity to bortezomib (Figure 2C). Using an in vivo model to help mimic the microenvironment's effects on UPP activity, we found that RPMI 8226/TJP1 shRNA tumors were less sensitive to bortezomib than RPMI 8226/control shRNA tumors (Figure 2D, left panel). On the other hand, treatment of mice with MOLP-8/TJP1 cells resulted in a greater reduction in tumor growth (Figure 2D, right). Finally, because myeloma is characterized by lytic bony lesions, we compared mice bearing RPMI 8226/TJP1 shRNA cells with those bearing control shRNAs. Bortezomib treatment reduced lytic disease in both, but was more marked in RPMI 8226/control shRNA cells (Figure 2E, left). Moreover, mice with RPMI 8226/TJP1 shRNA cells treated with bortezomib had a lower bone volume density than controls (Figure 2E, right), consistent with a resistant phenotype in the presence of lower TJP1 levels.

TJP1 Influences Proteasome Activity

To probe the mechanisms by which TJP1 influenced PI sensitivity, we compared RPMI 8226/TJP1 shRNA cells with controls. Upregulation of major histocompatibility (MHC) class II gene expression was the most significant difference by GSEA (Figures S1F and S1G; Table S2), and correlated with increased human leukocyte antigen (HLA)-DPB1 protein levels (Figure 3A). This reminded us that two catalytic immunoproteasome subunits, proteasome subunit β-type (PSMB)-8 (low molecular mass protein [LMP]-7), which encodes the chymotrypsin-like (ChT-L) proteasome activity, and PSMB9, or LMP2, are in the MHC class II region (Orlowski and Wilk, 2000). Both the constitutive proteasome and the immunoproteasome contribute to proteasome activity, and are inhibited by bortezomib and carfilzomib (Moreau et al., 2012; Ortiz-Navarrete et al., 1991). We therefore considered that TJP1 enhanced PI sensitivity by reducing LMP7 and LMP2, thereby decreasing proteasome capacity. Indeed, TJP1 suppression in RPMI 8226 and U266 cells increased LMP7 and LMP2 expression, while its overexpression in MOLP-8 cells reduced their levels (Figure 3B). Because the ChT-L activity is the rate-limiting step in proteolysis, we measured the influence of TJP1 and found a direct relationship, with higher LMP7 levels being associated with higher proteasome ChT-L activity, while lower ChT-L activity was seen in

cells with decreased LMP7 (Figure 3C). Similarly, in mESCs, *Tjp1* KO was associated with higher LMP7 and LMP2 levels (Figure 3D) and greater ChT-L activity (Figure 3E), while reintroduction of TJP1 into KO mESCs reduced the ChT-L activity (Figure 3E). Finally, studies of the proteasome load showed no consistent differences with TJP1 suppression (Figure 3F), suggesting that TJP1 impacts only upon proteasome capacity.

EGFR/JAK/STAT Signaling Links TJP1 to Proteasome Activity and PI Sensitivity

Studies in colorectal and pancreatic cancer models have suggested that TJP1 interacts with the epidermal growth factor receptor (EGFR) (Kaihara et al., 2003; Takai et al., 2005), and we therefore evaluated phospho-EGFR levels in myeloma. When TJP1 was suppressed, phospho-EGFR levels increased, while they declined when TJP1 was overexpressed (Figure 4A). Downstream EGFR signaling flows through Janus kinases (JAKs) and Signal transducers and activators of transcription (STATs). TJP1 suppression increased phospho-JAK1 levels, whereas decreased JAK1 activation was seen with TJP1 overexpression (Figure 4B). Moreover, STAT3 activation was enhanced by TJP1 suppression and reduced by TJP1 overexpression (Figure 4C).

STAT3 plays a key role in malignancies through many targets, and we noted that MHC class II genes induced by TJP1 suppression, including *HLA-DPB1*, and *LMP7* and *LMP2*, had nearby consensus STAT3 binding sites (Table S4). Myeloma cells in which STAT3 was suppressed had decreased HLA-DPB1 (Figure 5A) and LMP7 and LMP2 levels (Figure 5B), which correlated with a reduction in ChT-L activity (Figure 5C). Given their lower capacity for protein turnover, these cells were more sensitive to PIs (Figure 5D). Finally, since STAT3 activation could reduce sensitivity through multiple mechanisms, we overexpressed LMP7 or LMP2, and found that this by itself reduced bortezomib sensitivity (Figure 5E). Thus, these data support a model in which TJP1 suppressed EGFR/JAK1/STAT3 signaling, which reduced expression of the catalytic LMP7 and LMP2 subunits, thereby reducing proteasome capacity and making cells more PI sensitive (Figure 5F).

To better understand the mechanisms by which TJP1 expression reduced EGFR/JAK/STAT signaling, we first performed coimmunoprecipitation. An anti-TJP1 antibody co-precipitated total EGFR (Figure S2A), and an anti-total EGFR antibody co-precipitated TJP1 (Figure S2B). When this was repeated with an anti-phospho-EGFR antibody, TJP1 precipitation revealed no phosphorylated EGFR (Figure S2C), while phospho-EGFR precipitation did not pull down TJP1 (Figure S2D). Next, since STAT3 mediates signaling through interleukin-6 (IL-6), and insulin-like growth factor 1 (IGF-1) signaling is important in myeloma biology, we examined their receptors. TJP1 immunoprecipitation did not pull down the IL-6 receptor (IL-6R) (Figure S2E), but we did detect the IGF-1 receptor (IGF-1R) (Figure S2F). To further clarify which was important in modulating PI sensitivity, we evaluated the influence of their respective ligands. While EGF enhanced the expression levels of LMP7 and LMP2, IGF-1 and IL-6 did not (Figure 6A), and only EGF enhanced proteasome ChT-L activity and, therefore, proteasome capacity (Figure 6B). Finally, since EGF/EGFR signaling has been extensively studied in epithelial malignancies, we evaluated EGF-sensitive A549 adenocarcinoma cells. As in myeloma cells, EGF enhanced LMP7 and LMP2 expression

(Figure 6C) and proteasome capacity (Figure 6D), and preserved viability in the face of bortezomib (Figure 6E).

Targeting EGF/EGFR Signaling in Myeloma

The relevance of EGF/EGFR signaling is not well established in myeloma, so we first looked at the Multiple Myeloma Genomics Portal's Mayo Clinic Cell Line dataset and found that EGFR mRNA is expressed in myeloma cell lines (Figure S3A). Also, qPCR confirmed that it was at levels seen in some epithelial tumor lines (Figure S3B). Expression profiles of myeloma samples from newly diagnosed and relapsed/refractory myeloma patients showed that EGFR is plausibly expressed in primary cells (Figure S3C). Moreover, RNA-sequencing data showed that EGFR mRNA was detectable in half of the patients (Figure S3D). While the EGFR expression level was lower than that of other genes expressed in myeloma, it was consistent with the lower EGFR levels seen in other hematologic malignancies from The Cancer Genome Atlas (Figure S3E). Furthermore, EGFR protein was detectable in lysates (Figure 7A) and on the surface (Figure S4A) of some myeloma cell lines, albeit at lower levels than in epithelial cells. The same was true in patient-derived primary sample plasma cell isolates studied by western blotting (Figure 7B) and flow cytometry (Figure S4B). Next, we exposed RPMI 8226 (Figure 7C) and U266 cells (Figure 7D) to the EGFR inhibitor erlotinib, which reduced phospho-STAT3, LMP7, and LMP2 levels, and increased sensitivity to bortezomib. We then examined ten primary samples for which we had sufficient cells to perform both flow cytometry and cell viability studies. Compared with controls, seven samples had ≥10% of cells that were $CD138^+$ and $EGFR^+$ (Figure S5), such as sample 14 (Figure 7E), and we treated all these samples with vehicle, erlotinib, bortezomib, or the combination. Addition of erlotinib to bortezomib enhanced the reduction in viability to some extent in all of the samples tested (Figures 7F and S6) in a manner influenced by the erlotinib concentration. Treatment of the primary samples with bortezomib showed a direct relationship between viability and EGFR expression levels (Figure 7G), with samples having greater EGFR expression retaining more viability after bortezomib. Moreover, although erlotinib enhanced bortezomib's efficacy in samples that were below or above the median EGFR expression (Figure 7H) ($p < 0.001$), the differences were greater in samples with higher EGFR levels ($p < 0.001$). Finally, $EGFR^-$ Jurkat leukemic T cells were prepared with a control shRNA or TJP1-supressing shRNAs. When treated with bortezomib, no difference was seen in their viability (Figure S7), supporting the hypothesis that EGFR was necessary for TJP1-mediated modulation of PI sensitivity.

TJP1 Is a Biomarker of PI Sensitivity

We next examined whether TJP1 expression could identify patients most likely to benefit from bortezomib-based therapy. First, we evaluated the outcomes of newly diagnosed patients treated with Total Therapy III (TT3), which utilized bortezomib (Table S5). Patients who received TT3a were divided into tertiles based on TJP1 expression levels, and progression-free survival (PFS) in the first (lowest) tertile was significantly lower than the other two tertiles (Figure 8A). Since the outcomes in tertiles 2 and 3 were similar, these were combined and compared with the first, which again showed an inferior PFS (Figure 8B). Data from TT3b were also examined, and patients in tertiles 2 and 3 again had superior outcomes (Figure 8C). In that multi-agent regimens were used in TT3, it was difficult to

conclude that TJP1 can be used specifically as a PI biomarker, and we returned to the clinically annotated bortezomib datasets. Patients who achieved a response after bortezomib across multiple studies had significantly higher TJP1 expression ($p = 0.000246$ and $p = 0.00922$ for the two TJP1 probes; Figure 8D), as expected, since this was how we had initially identified TJP1. Importantly, no difference was seen in TJP1 expression between responders and nonresponders to dexamethasone. As a final test, we analyzed the influence of TJP1 on time to progression (TTP), which was the primary end point for the bortezomib studies. Patients in TJP1 tertile 1 had the shortest TTP, those in tertile 3 had the longest, and those in the second were intermediate (Table S6). Once again, when tertiles 2 and 3 were combined, they had a significantly longer TTP than tertile 1 (Figure 8E).

Finally, to further evaluate the physiologic relevance of our findings, we performed GSEA of the TT3 database to identify pathways that correlated with TJP1 expression, and found several gene sets relevant to EGFR with significant positive enrichment (Table S7). One was AMIT_EGF_RESPONSE_60_MCF10A (Figure S8A), which included genes induced in MCF10A cells by EGF that functioned to attenuate growth factor signaling (Amit et al., 2007). Another included KOBAYASHI_EGFR_SIGNALING_24HR_UP (Figure S8B), which contained genes upregulated in non-small cell lung cancer T790M-mutant H1975 cells resistant to the EGFR inhibitor gefitinib (Kobayashi et al., 2006). The most highly positively enriched set was COLDREN_GEFITINIB_RESISTANCE_DN (Figure S8C), which included genes downregulated in non-small cell lung carcinoma cell lines resistant to gefitinib (Coldren et al., 2006). Importantly, analysis of the Millennium Pharmaceuticals database also identified the COLDREN_GEFITINIB_RESISTANCE_DN gene set as correlating to TJP1 expression (Table S8). Then, using Gene Signature Survival Analysis (GSSA) (our unpublished data), which finds signatures whose expression levels correlate significantly with outcomes in cancer datasets, we analyzed the TT3 database. The EGFR-related gene set KOBAYASHI_EGFR_SIGNALING_24HR_DN had a significant negative correlation with survival duration determined by a univariate Cox analysis of the signature score ($p = 3.28 \times 10^{-6}$). Using a permutation-based approach to correct for the fact that even random signatures often have univariate significant correlation when tested in isolation (Starmans et al., 2011; Venet et al., 2011), we obtained a permutation-corrected significance p value of 0.002, which was further corrected for false discovery, giving a q value of 0.05594. A nominally significant result was also obtained with a log-rank test, which was used to divide patients at the point of most significant difference (Figure S8D). Taken together, the data argue that TJP1 expression in primary myeloma cells is associated with physiologically relevant inhibition of EGFR signaling, and that this has a positive influence on patient outcomes.

DISCUSSION

Chemotherapeutics against myeloma are currently selected on an empirical basis, with patients typically receiving the regimens that have the highest response rates to which they have access. A more personalized treatment approach will require prospective validation of biomarkers that would identify patients most likely to benefit from certain drug classes, as well as those with resistant disease, which could improve outcomes, reduce toxicities, and save healthcare resources.

A recent study suggested that one pathway of bortezomib resistance was the emergence of XBP1s^{-} plasma cell precursors that were de-committed to immunoglobulin synthesis (Leung-Hagesteijn et al., 2013). Were this the only mode of resistance then all patients with refractory disease should have oligoor non-secretory myeloma, but clinically this is not the case, suggesting that other mechanisms contribute. Interestingly, our data show that low TJP1 expression can reduce the load/capacity ratio in the same direction as loss of XBP1s, although by enhancing proteasome capacity. However, our findings suggest that these mechanisms are distinct, given the lack of overlap between the TJP1 and XBP1s signatures. Indeed, our analysis did not detect XBP1 as a resistance marker, which may be because the analysis by Leung-Hagesteijn et al. (2013) was limited to a subset of only 13 patients with complete remission and 41 with progressive disease, while we analyzed the entire dataset of 171 patients.

The reduction of EGFR/JAK1/STAT3 signaling by TJP1 is likely due to a direct interaction between TJP1 and EGFR. There are known interactions between EGFR and the Na^{+}/H^{+} exchanger regulatory factor (NHERF) (Borg et al., 2000), and between EGFR2 and the Erbb2 interacting protein (ERBIN) (Borg et al., 2000). These occur through the ERBIN and NHERF PDZ (postsynaptic density protein, *Drosophila* disc large tumor suppressor, and ZO-1) domains and, notably, TJP1, also known as zona occludens 1 (ZO-1), contains three PDZ domains. Reduced EGFR signaling could therefore result from preferential binding of TJP1 to inactive EGFR, which would prevent receptor dimerization and autophosphorylation. Moreover, ERBIN expression reduces EGFR2 activation by restricting EGFR2 to the basolateral membrane of epithelial cells (Borg et al., 2000), TJP1 may have a similar effect on EGFR. PDZ-domain proteins have been described to interact with IGF-1R (Ligensa et al., 2001), and we did find evidence that TJP1 may indeed bind IGF-1R. Moreover, initial studies show that TJP1 expression reduces Akt activation (data not shown), which could be due to an impact on signaling from IGF-1R. Therefore, we cannot rule out the possibility that decreased TJP1 expression may mediate bortezomib resistance in part through Akt activation (Mitsiades et al., 2002), and we are investigating this possibility. However, we did show that LMP7 and LMP2 expression was sufficient to confer resistance by increasing proteasome capacity, and that EGFR/JAK/STAT3 modulated LMP7 and LMP2 levels. Thus, especially given that only EGF, and not IGF-1, induced LMP7 and LMP2 expression, our data support the conclusion that resistance due to enhanced proteasome capacity is mediated mainly through TJP1 and its effects on EGFR/JAK/STAT3/LMP7/2.

Our data showing that activation of LMP7/2 expression occurs through EGFR but not IL-6R are interesting, since both receptors signal through STAT3. However, this is consistent with other studies showing that JAK/STAT activation via different receptors can lead to different outputs. For example, IL-6R and IL-10R both activate STAT3, but only IL-10R induces anti-inflammatory response genes, possibly due to different durations of STAT3 activation (Murray, 2007). Similarly, IL-2 and IL-15, both of which signal through the same receptor, induce different downstream phenotypes, which has also been ascribed to their ability to modulate different strengths and durations of receptor activation (Arneja et al., 2014). We therefore hypothesize that perhaps EGFR-mediated STAT3 activation kinetics differ from those of IL-6 to account for their differential effect on proteasome subunit induction.

TJP1 may also influence PI sensitivity through other mechanisms, since MHC class II region genes implicated in multidrug resistance (Deverson et al., 1990) may reduce the activity of bortezomib (O'Connor et al., 2013). In addition, STAT3 suppression could decrease levels of myeloid cell leukemia-1, which plays a key role in bortezomib-mediated apoptosis (Podar et al., 2008). These potential mechanisms suggest that it is worth evaluating TJP1 in resistance to other chemotherapeutics, and possibly in other diseases as well. Indeed, the ability of TJP1 to modulate the efficacy of other drugs is suggested by the greater influence of TJP1 on outcomes of newly diagnosed patients treated with TT3 than on single-agent bortezomib. Another possibility is that TJP1 plays a greater role in primary, or innate, resistance in less heavily treated myeloma. This is supported by the finding that its impact on PFS was greater in newly diagnosed patients. In relapsed/refractory disease, additional secondary, or acquired, resistance factors may contribute and TJP1 levels may already be lowered by the time of the development of refractory disease. Indeed, our models of BR myeloma suggest that this is the case, since they generally expressed lower TJP1 levels than drug-naive cells. In addition, our current clinical data analyses support a role for TJP1 as a biomarker of bortezomib sensitivity, but the pre-clinical studies suggest that it should be similarly helpful as a marker for other PIs such as carfilzomib. To test this possibility, we will be evaluating TJP1 expression levels in the context of an SWOG-led intergroup study (S1304) of carfilzomib with dexamethasone. In addition, it is possible that other pathways contribute to the ability of TJP1 to modulate PI sensitivity. For example, we recently found that PI resistance was also associated with activation of the nuclear factor (erythroid-derived 2)-like (NRF2) and proteasome maturation protein (POMP) axis (Li et al., 2015). LMP7 and LMP2 are inactive alone, and cannot bind bortezomib or carfilzomib until they are assembled into proteasome β-subunit rings and then active proteasomes, so the NRF2/POMP axis may cooperate with TJP1 loss in enhancing proteasome capacity. However, NRF2 and POMP expression was not predictive of patient outcomes, suggesting that it is the availability of LMP7 and LMP2 that are rate limiting, and that the TJP1/EGFR pathway is more important in determining PI sensitivity.

Signaling through the EGF/EGFR axis has not been extensively examined in the myeloma context, but our results demonstrate that EGFR is expressed by plasma cells. These findings are consistent with earlier reports showing that EGFR was expressed in the majority of multiple myeloma cell lines and primary samples tested by qPCR (Mahtouk et al., 2004, 2005). Furthermore, EGF has been shown to induce proliferation of myeloma cells that express high STAT3 levels (French et al., 2002), and anti-EGFR antibodies were shown to slow the growth of myeloma cell lines (Wang et al., 2002). More recently, Walker et al. (2013) identified an EGFR translocation in a patient's myeloma cells, and sequencing has shown that EGFR mutations can be detected in primary myeloma samples (Lohr et al., 2014; Mulligan et al., 2014), albeit at a low frequency. Notably, the report from Mulligan et al. was on the same patients whose gene-expression profile (GEP) we had analyzed to identify TJP1, to determine that its expression correlated with signatures of EGFR inhibition, and to note that EGFR signaling was associated with an inferior clinical outcome. Thus, these data together support the statement that EGF/EGFR signaling is physiologically relevant to myeloma in the absence of EGFR-activating mutations through an influence on proteasome capacity. Moreover, these data suggest possibly fruitful directions for future exploration of

approaches that could overcome the impact of decreased TJP1 expression upon the EGFR pathway. Since low TJP1 levels result in greater plasma cell proteasome content, PI resistance in this setting could be overcome by using higher-dose PI regimens. Also, in patients whose myeloma expresses low TJP1, EGFR and/or JAK inhibitors may enhance PI sensitivity, especially in patients whose plasma cells have a high surface EGFR expression. Ongoing and planned studies will further address these possibilities as we fully explore the biology of this pathway in myeloma.

EXPERIMENTAL PROCEDURES

Cell Culture

Human drug-naive and BR cells were cultured as previously described (Kuhn et al., 2012). Cell-line authentication was performed by the MD Anderson Cell Line Characterization Core using short-tandem-repeat profiling. Primary cells were obtained from patients undergoing bone marrow aspiration after they had provided informed consent in compliance with the Declaration of Helsinki according to a protocol approved by The MD Anderson Cancer Center Institutional Review Board. Primary cells were purified by positive selection using magnetic-activated cell sorting with CD138 microbeads (Miltenyi Biotec).

Gene-Expression Profiling and Analysis of Clinical Datasets

Clinically annotated GEP datasets from bortezomib trials are available at GEO: GSE9782. GEP data from bortezomib-sensitive and -resistant ANBL-6 and KAS-6/1 myeloma cells (Kuhn et al., 2012), which were used to identify *TJP1*, are available at GEO: GSE52369.

Quantitative Real-Time PCR

Measurements of mRNA levels for genes of interest and their controls were performed by quantitative real-time PCR as previously described (Bjorklund et al., 2014).

Western Blotting and Immunoprecipitation

Protein lysates were prepared and analyzed as described previously (Bjorklund et al., 2014).

Cell-Cycle Assays

Induction of apoptosis was followed by measuring the proportion of cells with a sub-G_1 DNA content by flow cytometry as previously described (Jones et al., 2011).

Cell Viability Assays

The tetrazolium reagent WST-1 was used to determine cell viability according to the manufacturer's protocol and as previously described (Bjorklund et al., 2011, 2014).

Proteasome Activity Measurements

The chymotrypsin-like activity of the proteasome was determined as described previously (Kuhn et al., 2012).

Murine Models

Studies involving mice were conducted in accordance with federal and institutional guidelines under protocols approved by The MD Anderson Cancer Center Animal Care and Use Facility, and all mice were maintained in American Association of Laboratory Animal Care-accredited facilities. Mice with severe combined immunodeficiency (SCID) were purchased from Harlan Laboratories. An in vivo xenograft model based on RPMI 8226 cells was developed in immunodeficient mice by injecting RPMI 8226/control shRNA, or RPMI 8226/TJP1 shRNA cells. Myeloma xenograft tumors were generated by injecting $2–5 \times 10^6$ cells resuspended in Matrigel (BD Biosciences) subcutaneously in the left and right flank of female SCID beige mice. Similar studies compared the sensitivity to bortezomib or carfilzomib of MOLP-8/vector with MOLP-8/TJP1 cells, which were generated by injecting 1.5×10^7 cells resuspended in Matrigel subcutaneously. Mice were randomized into treatment groups based on tumor volume. Average tumor volume in treatment groups at the time of randomization and start of treatment was 100–250 mm^3 measured using the equation volume = (length × $width^2$)/2. Bortezomib (0.5 mg/kg) injections were given through the intraperitoneal route in a solution of 10 mg/ml mannitol in saline twice weekly for 2 weeks.

For studies of myeloma bone disease, a total of 1×10^6 RPMI 8226/control shRNA or RPMI 8226/TJP1 shRNA cells were injected intravenously into 6- to 8-week-old SCID mice. To measure the size of lytic bone lesions, we obtained radiographs with a Faxitron X-ray cabinet (Faxitron X-ray). The histomorphometric analysis was performed on a Leica Quantimet Q570 image analyzer. Cortical thickness is the mean of external and internal cortical thickness, expressed in micrometers. Trabecular bone volume (BV) is the amount of trabecular bone within the spongy space (expressed as a percentage). The ratio of BV to total volume (TV) is derived from measurements of bone area (B.Ar) and cancellous tissue area (T.Ar) and is expressed as BV/TV = B.Ar/T.Ar.

Supplementary Material

Refer to Web version on PubMed Central for supplementary material.

Acknowledgments

This work was supported by The MD Anderson Cancer Center SPORE in Multiple Myeloma (P50 CA142509) and The MD Anderson Cancer Center Support Grant (P30 CA016672). L.Y. would like to acknowledge support from the Priority Academic Program Development of Jiangsu Higher Education Institutions and the National Natural Science Foundation of China (81272476). X.Z. would like to acknowledge support from the National Natural Science Foundation of China (81201861), and a Research Fellow Award from the Multiple Myeloma Research Foundation. B.B., S.Z.U., Q.Z., and J.C. would like to acknowledge support from the National Cancer Institute (P01 CA055819). S.C. would like to acknowledge support from the Italian Association for Cancer Research (AIRC, Investigator Grant 14691 and Special Program Molecular Clinical Oncology 5 per mille no. 9965). R.Z.O., the Florence Maude Thomas Cancer Research Professor, would also like to acknowledge support from the National Cancer Institute (U10 CA032102, R01 CA184464, CA194264), the MD Anderson Cancer Center High Risk Multiple Myeloma Moon Shot, and thank the Brock Family Myeloma Research Fund, the Yates Ortiz Myeloma Fund, the Jay Solomon Myeloma Research Fund, and the Diane & John Grace Family Foundation. G.M., B.L., and D.W.E. are employees of Millennium: The Takeda Oncology Company, which developed and markets bortezomib. R.Z.O. has served on advisory boards for Millennium: The Takeda Oncology Company, which developed and markets bortezomib, and for Onyx Pharmaceuticals, which developed and markets carfilzomib, and has received research support from these firms for other clinical and laboratory projects. B.B. has received research funding from Celgene Corporation and Millennium, is a consultant to Celgene and Millennium, and is a co-inventor on patents and patent applications related to the use of gene-expression profiling in cancer medicine that have been licensed to Myeloma Health, LLC. G.M., B.L., and D.W.E. were employees and shareholders of Takeda Pharmaceuticals USA,

Inc., which developed and markets bortezomib. B.B. has received research funding from, and is a research consultant to Takeda Pharmaceuticals USA, Inc., and is a co-inventor on patents and patent applications related to the use of gene-expression profiling in cancer medicine that have been licensed to Signal Genetics. S.Z.U., J.J.S., and R.Z.O. have served on advisory boards for Takeda Pharmaceuticals USA, Inc., and for Amgen, which developed and markets carfilzomib, and S.Z.U. and R.Z.O. have received research funding from these firms. S.Z.U. has served on speaker's bureaus for Takeda Pharmaceuticals USA, Inc., and for Amgen.

REFERENCES

Amit I, Citri A, Shay T, Lu Y, Katz M, Zhang F, Tarcic G, Siwak D, Lahad J, Jacob-Hirsch J, et al. A module of negative feedback regulators defines growth factor signaling. Nat. Genet. 2007; 39:503–512. [PubMed: 17322878]

Arneja A, Johnson H, Gabrovsek L, Lauffenburger DA, White FM. Qualitatively different T cell phenotypic responses to IL-2 versus IL-15 are unified by identical dependences on receptor signal strength and duration. J. Immunol. 2014; 192:123–135. [PubMed: 24298013]

Bianchi G, Oliva L, Cascio P, Pengo N, Fontana F, Cerruti F, Orsi A, Pasqualetto E, Mezghrani A, Calbi V, et al. The proteasome load versus capacity balance determines apoptotic sensitivity of multiple myeloma cells to proteasome inhibition. Blood. 2009; 113:3040–3049. [PubMed: 19164601]

Bjorklund CC, Ma W, Wang ZQ, Davis RE, Kuhn DJ, Kornblau SM, Wang M, Shah JJ, Orlowski RZ. Evidence of a role for activation of Wnt/beta-catenin signaling in the resistance of plasma cells to lenalidomide. J. Biol. Chem. 2011; 286:11009–11020. [PubMed: 21189262]

Bjorklund CC, Baladandayuthapani V, Lin HY, Jones RJ, Kuiatse I, Wang H, Yang J, Shah JJ, Thomas SK, Wang M, et al. Evidence of a role for CD44 and cell adhesion in mediating resistance to lenalidomide in multiple myeloma: therapeutic implications. Leukemia. 2014; 28:373–383. [PubMed: 23760401]

Borg JP, Marchetto S, Le Bivic A, Ollendorff V, Jaulin-Bastard F, Saito H, Fournier E, Adelaide J, Margolis B, Birnbaum D. ERBIN: a basolateral PDZ protein that interacts with the mammalian ERBB2/HER2 receptor. Nat. Cell Biol. 2000; 2:407–414. [PubMed: 10878805]

Cenci S, Mezghrani A, Cascio P, Bianchi G, Cerruti F, Fra A, Lelouard H, Masciarelli S, Mattioli L, Oliva L, et al. Progressively impaired proteasomal capacity during terminal plasma cell differentiation. EMBO J. 2006; 25:1104–1113. [PubMed: 16498407]

Coldren CD, Helfrich BA, Witta SE, Sugita M, Lapadat R, Zeng C, Baron A, Franklin WA, Hirsch FR, Geraci MW, Bunn PA Jr. Baseline gene expression predicts sensitivity to gefitinib in non-small cell lung cancer cell lines. Mol. Cancer Res. 2006; 4:521–528. [PubMed: 16877703]

Deverson EV, Gow IR, Coadwell WJ, Monaco JJ, Butcher GW, Howard JC. MHC class II region encoding proteins related to the multidrug resistance family of transmembrane transporters. Nature. 1990; 348:738–741. [PubMed: 1979660]

French JD, Tschumper RC, Jelinek DF. Analysis of IL-6-mediated growth control of myeloma cells using a gp130 chimeric receptor approach. Leukemia. 2002; 16:1189–1196. [PubMed: 12040452]

Hideshima T, Anderson KC. Biologic impact of proteasome inhibition in multiple myeloma cells–from the aspects of preclinical studies. Semin. Hematol. 2012; 49:223–227. [PubMed: 22726545]

Jones RJ, Baladandayuthapani V, Neelapu S, Fayad LE, Romaguera JE, Wang M, Sharma R, Yang D, Orlowski RZ. HDM-2 inhibition suppresses expression of ribonucleotide reductase subunit M2, and synergistically enhances gemcitabine-induced cytotoxicity in mantle cell lymphoma. Blood. 2011; 118:4140–4149. [PubMed: 21844567]

Kaihara T, Kawamata H, Imura J, Fujii S, Kitajima K, Omotehara F, Maeda N, Nakamura T, Fujimori T. Redifferentiation and ZO-1 reexpression in liver-metastasized colorectal cancer: possible association with epidermal growth factor receptor-induced tyrosine phosphorylation of ZO-1. Cancer Sci. 2003; 94:166–172. [PubMed: 12708492]

Kobayashi S, Shimamura T, Monti S, Steidl U, Hetherington CJ, Lowell AM, Golub T, Meyerson M, Tenen DG, Shapiro GI, Halmos B. Transcriptional profiling identifies cyclin D1 as a critical downstream effector of mutant epidermal growth factor receptor signaling. Cancer Res. 2006; 66:11389–11398. [PubMed: 17145885]

Kuhn DJ, Berkova Z, Jones RJ, Woessner R, Bjorklund CC, Ma W, Davis RE, Lin P, Wang H, Madden TL, et al. Targeting the insulin-like growth factor-1 receptor to overcome bortezomib resistance in preclinical models of multiple myeloma. Blood. 2012; 120:3260–3270. [PubMed: 22932796]

Kyle RA, Rajkumar SV. Multiple myeloma. Blood. 2008; 111:2962–2972. [PubMed: 18332230]

Leung-Hagesteijn C, Erdmann N, Cheung G, Keats JJ, Stewart AK, Reece DE, Chung KC, Tiedemann RE. Xbp1s-negative tumor B cells and pre-plasmablasts mediate therapeutic proteasome inhibitor resistance in multiple myeloma. Cancer Cell. 2013; 24:289–304. [PubMed: 24029229]

Li B, Fu J, Chen P, Ge X, Li Y, Kuiatse I, Wang H, Whang H, Zhang X, Orlowski RZ. The nuclear factor (erythroid-derived 2)-like 2 and proteasome maturation protein axis mediates bortezomib resistance in multiple myeloma. J. Biol. Chem. 2015; 290:29854–29868. [PubMed: 26483548]

Ligensa T, Krauss S, Demuth D, Schumacher R, Camonis J, Jaques G, Weidner KM. A PDZ domain protein interacts with the C-terminal tail of the insulin-like growth factor-1 receptor but not with the insulin receptor. J. Biol. Chem. 2001; 276:33419–33427. [PubMed: 11445579]

Lohr JG, Stojanov P, Carter SL, Cruz-Gordillo P, Lawrence MS, Auclair D, Sougnez C, Knoechel B, Gould J, Saksena G, et al. Widespread genetic heterogeneity in multiple myeloma: implications for targeted therapy. Cancer Cell. 2014; 25:91–101. [PubMed: 24434212]

Mahtouk K, Jourdan M, De Vos J, Hertogh C, Fiol G, Jourdan E, Rossi JF, Klein B. An inhibitor of the EGF receptor family blocks myeloma cell growth factor activity of HB-EGF and potentiates dexamethasone or anti-IL-6 antibody-induced apoptosis. Blood. 2004; 103:1829–1837. [PubMed: 14576062]

Mahtouk K, Hose D, Reme T, De Vos J, Jourdan M, Moreaux J, Fiol G, Raab M, Jourdan E, Grau V, et al. Expression of EGF-family receptors and amphiregulin in multiple myeloma. Amphiregulin is a growth factor for myeloma cells. Oncogene. 2005; 24:3512–3524. [PubMed: 15735670]

Mitsiades N, Mitsiades CS, Poulaki V, Chauhan D, Fanourakis G, Gu X, Bailey C, Joseph M, Libermann TA, Treon SP, et al. Molecular sequelae of proteasome inhibition in human multiple myeloma cells. Proc. Natl. Acad. Sci. USA. 2002; 99:14374–14379. [PubMed: 12391322]

Moreau P, Richardson PG, Cavo M, Orlowski RZ, San Miguel JF, Palumbo A, Harousseau JL. Proteasome inhibitors in multiple myeloma: 10 years later. Blood. 2012; 120:947–959. [PubMed: 22645181]

Mulligan G, Lichter DI, Di Bacco A, Blakemore SJ, Berger A, Koenig E, Bernard H, Trepicchio W, Li B, Neuwirth R, et al. Mutation of NRAS but not KRAS significantly reduces myeloma sensitivity to single-agent bortezomib therapy. Blood. 2014; 123:632–639. [PubMed: 24335104]

Murray PJ. The JAK-STAT signaling pathway: input and output integration. J. Immunol. 2007; 178:2623–2629. [PubMed: 17312100]

O'Connor R, Ooi MG, Meiller J, Jakubikova J, Klippel S, Delmore J, Richardson P, Anderson K, Clynes M, Mitsiades CS, O'Gorman P. The interaction of bortezomib with multidrug transporters: implications for therapeutic applications in advanced multiple myeloma and other neoplasias. Cancer Chemother. Pharmacol. 2013; 71:1357–1368. [PubMed: 23589314]

Orlowski RZ. Why proteasome inhibitors cannot ERADicate multiple myeloma. Cancer Cell. 2013; 24:275–277. [PubMed: 24029222]

Orlowski M, Wilk S. Catalytic activities of the 20 S proteasome, a multicatalytic proteinase complex. Arch. Biochem. Biophys. 2000; 383:1–16. [PubMed: 11097171]

Ortiz-Navarrete V, Seelig A, Gernold M, Frentzel S, Kloetzel PM, Hammerling GJ. Subunit of the '20S' proteasome (multicatalytic proteinase) encoded by the major histocompatibility complex. Nature. 1991; 353:662–664. [PubMed: 1922384]

Podar K, Gouill SL, Zhang J, Opferman JT, Zorn E, Tai YT, Hideshima T, Amiot M, Chauhan D, Harousseau JL, Anderson KC. A pivotal role for Mcl-1 in Bortezomib-induced apoptosis. Oncogene. 2008; 27:721–731. [PubMed: 17653083]

Shah JJ, Orlowski RZ. Proteasome inhibitors in the treatment of multiple myeloma. Leukemia. 2009; 23:1964–1979. [PubMed: 19741722]

Starmans MH, Fung G, Steck H, Wouters BG, Lambin P. A simple but highly effective approach to evaluate the prognostic performance of gene expression signatures. PLoS One. 2011; 6:e28320. [PubMed: 22163293]

Takai E, Tan X, Tamori Y, Hirota M, Egami H, Ogawa M. Correlation of translocation of tight junction protein Zonula occludens-1 and activation of epidermal growth factor receptor in the regulation of invasion of pancreatic cancer cells. Int. J. Oncol. 2005; 27:645–651. [PubMed: 16077912]

Venet D, Dumont JE, Detours V. Most random gene expression signatures are significantly associated with breast cancer outcome. PLoS Comput. Biol. 2011; 7:e1002240. [PubMed: 22028643]

Walker BA, Wardell CP, Johnson DC, Kaiser MF, Begum DB, Dahir NB, Ross FM, Davies FE, Gonzalez D, Morgan GJ. Characterization of IGH locus breakpoints in multiple myeloma indicates a subset of translocations appear to occur in pregerminal center B cells. Blood. 2013; 121:3413–3419. [PubMed: 23435460]

Wang YD, De Vos J, Jourdan M, Couderc G, Lu ZY, Rossi JF, Klein B. Cooperation between heparin-binding EGF-like growth factor and interleukin-6 in promoting the growth of human myeloma cells. Oncogene. 2002; 21:2584–2592. [PubMed: 11971193]

Xu J, Lim SB, Ng MY, Ali SM, Kausalya JP, Limviphuvadh V, Maurer-Stroh S, Hunziker W. ZO-1 regulates Erk, Smad1/5/8, Smad2, and RhoA activities to modulate self-renewal and differentiation of mouse embryonic stem cells. Stem Cells. 2012; 30:1885–1900. [PubMed: 22782886]

Highlights

- TJP1 expression is a biomarker of proteasome inhibitor sensitivity in myeloma
- Signaling through the TJP1/EGFR/JAK/STAT pathway influences proteasome capacity
- EGFR/JAK/STAT suppression induces chemosensitization to proteasome inhibitors

In Brief

Zhang et al. show that TJP1 enhances multiple myeloma sensitivity to proteasome inhibitors by reducing the expression of the immunoproteasome subunits LMP7 and LMP2 via suppression of EGFR/JAK1/STAT3 signaling, and that high TJP1 expression in patient myeloma cells correlates with better response to bortezomib.

Significance

Plasma cells are uniquely sensitive to proteasome inhibitors because their protein turnover capacity is reduced during differentiation. The current studies have identified a pathway involving TJP1, and signaling through EGFR/JAK1/STAT3, as important determinants of cellular proteasome capacity. In addition, low TJP1 expression was determined to be associated with, and to predict for, resistance to proteasome inhibitors pre-clinically and clinically. These findings provide a framework for the use of TJP1 as a biomarker to target proteasome inhibitor-based therapy to those patients who are most likely to benefit. Moreover, they provide a roadmap for translation of approaches targeting the EGFR/ JAK1/STAT3 pathway to enhance proteasome inhibitor sensitivity, and possibly overcome proteasome inhibitor resistance.

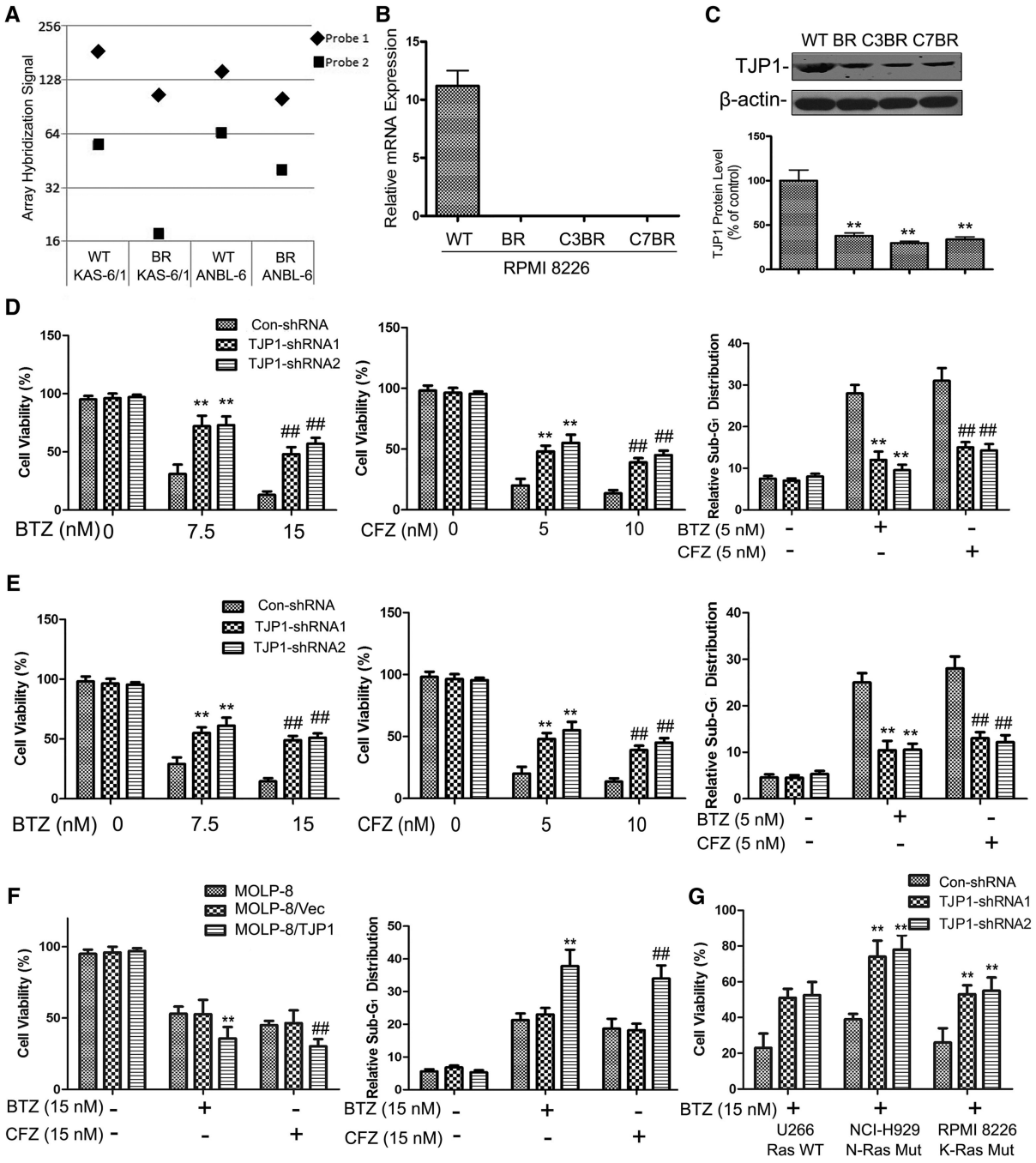

Figure 1. TJP1 Modulates PI Sensitivity in Myeloma

(A) Mean normalized fluorescence values are shown for TJP1 probes ILMN_2403006 (Probe 1) and ILMN_1691499 (Probe 2) from GEP comparing WT and BR KAS-6/1 and ANBL-6 cells.

(B) qPCR detected TJP1 mRNA levels in WT RPMI 8226 cells, pooled RPMI 8226 BR cells, and two single-cell BR subclones, C3BR and C7BR. Error bars represent the mean ± SD.

(C) TJP1 was detected by western blotting in the cells from (B) compared with a β-actin loading control. A representative blot from one of two independent experiments is shown, while the lower panel shows densitometry with the WT cells arbitrarily set at 100. **$p < 0.01$ compared with the WT controls after correction for β-actin using Student's t test. Error bars represent the mean ± SD.

(D and E) RPMI 8226 (D) and U266 (E) myeloma cells expressing a control shRNA (Con-shRNA) or shRNAs targeting TJP1 (shRNA1 and 2) were exposed to vehicle, bortezomib (BTZ), or carfilzomib (CFZ), and their viability (left and middle panels) and cell-cycle distribution (right) were evaluated after 24 hr. Data from triplicate experiments are expressed as the mean ± SE in relation to the vehicle control cells, which were arbitrarily set at 100%, and analyzed using Student's t test for all panels. Error bars represent the mean ± SD. A **$p < 0.01$; ##$p < 0.01$ in comparison with vehicle-treated controls.

(F) MOLP-8WT cells, or MOLP-8 cells containing a vector control (Vec), or the same vector from which TJP1 was overexpressed were analyzed for their sensitivity to BTZ and CFZ. Error bars represent the mean ± SD. ** and ## indicates $p < 0.01$ comparing TJP1-overexpression with vector control cells.

(G) U266, H929, and RPMI 8226 myeloma cell lines harboring WT or mutant KRAS or NRAS were transfected with shRNAs repressing TJP1, or a control shRNA. They were then exposed to bortezomib and analyzed as described in (D). Error bars represent the mean ± SD. ** indicate $p < 0.01$ comparing TJP1-shRNA with Con-shRNA cells.

See also Figure S1 and Tables S1–S3.

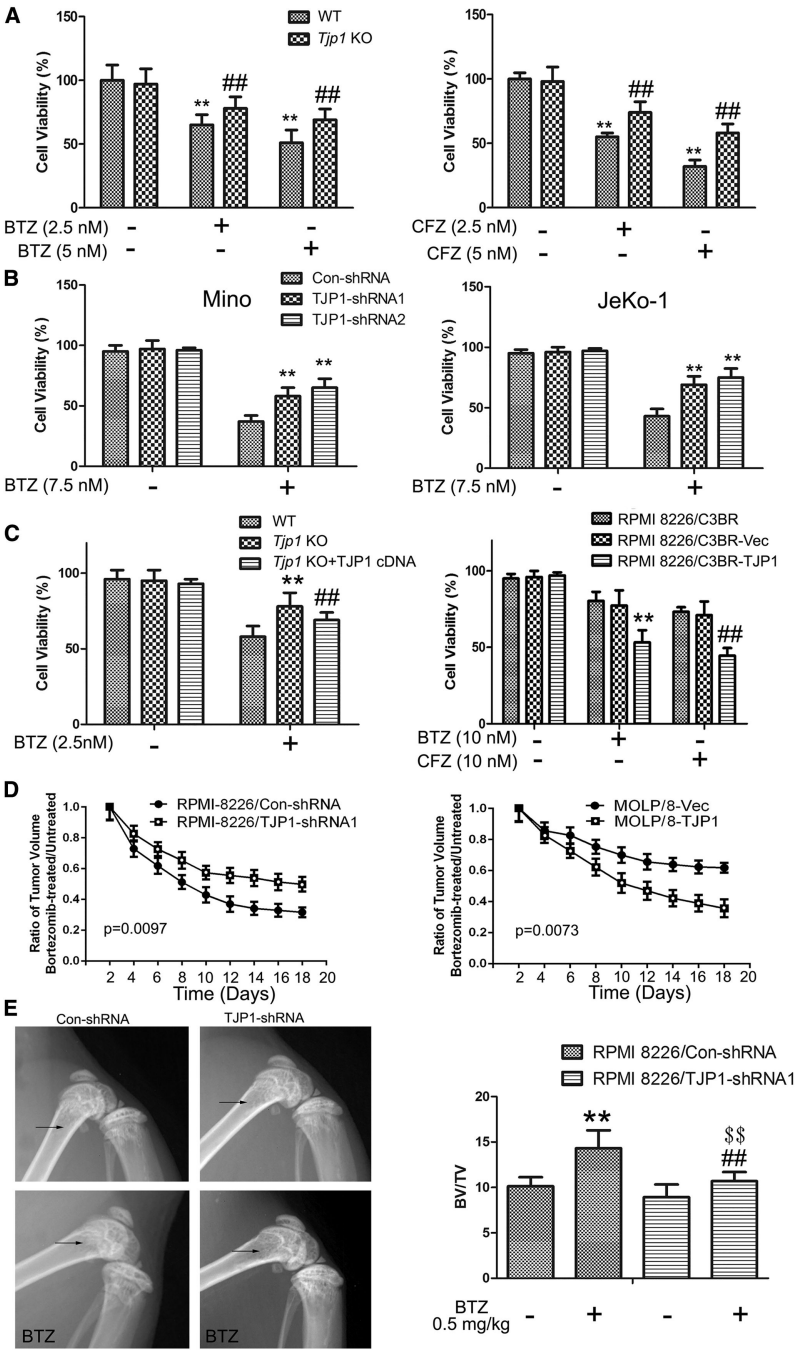

Figure 2. TJP1 Modulates PI Sensitivity in Myeloma

(A) WT mESCs or *Tjp1* KO mESCs were exposed to the indicated BTZ and CFZ for 72 hr and their cell viability was evaluated. Error bars represent the mean ± SD. ##p < 0.05 for comparisons between WT and *Tjp1* KO cells; **p < 0.05 for comparisons between treated and control cells.

(B) Mino (left panel) or JeKo-1 (right panel) MCL cells with Con-shRNA, or TJP1-shRNA1 or 2, were exposed to the indicated concentrations of vehicle or BTZ for 72 hr. Their

viability was then evaluated and analyzed as above. Error bars represent the mean ± SD. **p < 0.01 comparing TJP1-shRNA with Con-shRNA cells.

(C) *Tjp1* KO mESCs (left) or RPMI 8226 C3BR cells (right) were transfected with a vector that induced TJP1 expression, exposed to BTZ or CFZ for 72 hr, and compared with WT and vector cells. Error bars represent the mean ± SD. **p < 0.01, ##p < 0.05 comparing the viability of cells with TJP1 added back-treated with BTZ or CFZ with that of vector controls.

(D) Severe combined immunodeficiency (SCID) mice with flank xenografts of RPMI 8226/ConshRNA or TJP1-shRNA1 cells (left panel), or either MOLP-8/Vec or MOLP-8/TJP1 cells (right panel) were treated with vehicle or intraperitoneal BTZ on days 1 and 4 weekly. Tumors were measured on treatment days by a researcher who was blinded to the treatment assignments, and tumor volumes were calculated using (length × $width^2$)/2. The ratio of tumor size in the BTZ-treated to the vehicle-treated groups is plotted. Statistical analysis was performed using a one-way ANOVA followed by Dunnett's t test to compare tumor sizes on the last treatment day. Error bars represent the mean ± SD.

(E) RPMI 8226/Con-shRNA or TJP1-shRNA cells were injected into tail veins of SCID mice, which were then randomized to receive vehicle or 0.5 mg/kg bortezomib, and the development of bone disease was monitored radiographically. Representative lytic lesions in the femur of one mouse each in the control and TJP1 shRNA groups treated with bortezomib are shown (left), and indicated by arrows. Quantitative analysis of the radiographic images (right) shows the mineralized bone volume as the ratio of bone volume (BV) to total volume (TV) in distal femurs of mice bearing Con-shRNA or TJP1-shRNA myeloma cells treated with bortezomib. Error bars represent the mean ± SD. **p < 0.01 comparing RPMI 8226/Con-shRNA cells treated with BTZ treated with vehicle. $$p < 0.05 comparing 8226/TJP1-shRNA cells treated with BTZ treated with vehicle. ##p < 0.01 comparing 8226/TJP1-shRNA cells treated with BTZ with 8226/Con-shRNA cells treated with BTZ.

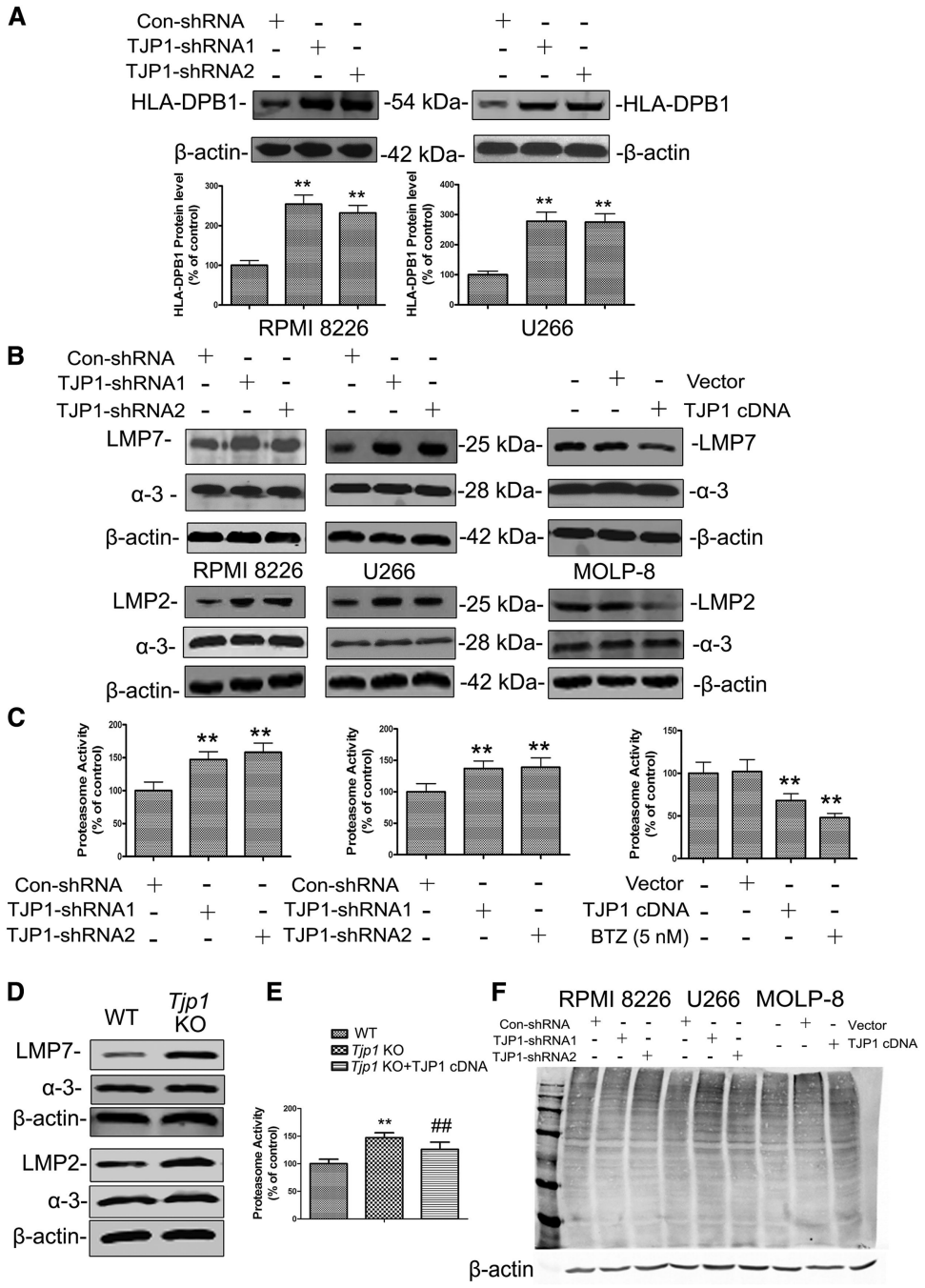

Figure 3. TJP1 and Proteasome Subunit Expression

(A) HLA DPB-1 expression in RPMI 8226 (left) or U266 (right) cells with Con-shRNA, or a TJP1 shRNA, was detected by western blotting. Beneath each blot, densitometry is shown in which Dpb-1 was normalized to β-actin, and the TJP1-shRNA data are then expressed in relation to controls arbitrarily set at 100. Error bars represent the mean ± SD. **$p < 0.01$ in comparison with ConshRNA.

(B) Expression of LMP7 and LMP2 in RPMI 8226 (left) and U266 cells (middle) with suppressed TJP1, or in MOLP-8 cells with overexpressed TJP1 (right). In addition to β-actin

as a loading control, expression of the α-3 proteasome subunit is shown since its gene is not located in the HLA region.

(C) Proteasome ChT-L activity was determined in RPMI 8226 (left), U266 (middle), and MOLP-8 cells (right). Data are from triplicate experiments in comparison to the respective controls set at 100%. Error bars represent the mean ± SD. **$p < 0.01$ compared with Con-shRNA cells.

(D) WT or *Tjp1* KO mESCs were probed to determine the expression of LMP7 and LMP2.

(E) ChT-L activity in WT, *Tjp1* KO, and *Tjp1* KO + TJP1 cDNA mESCs was evaluated in triplicate experiments. Student's t test was then performed. Error bars represent the mean ± SD. **$p < 0.01$; ##$p < 0.01$ in comparison with WT cells.

(F) Extracts from RPMI 8226, U266, and MOLP-8 cells engineered to express high or low levels of TJP1, and their respective controls, were subjected to western blotting with an anti-ubiquitin antibody, with β-actin as a loading control.

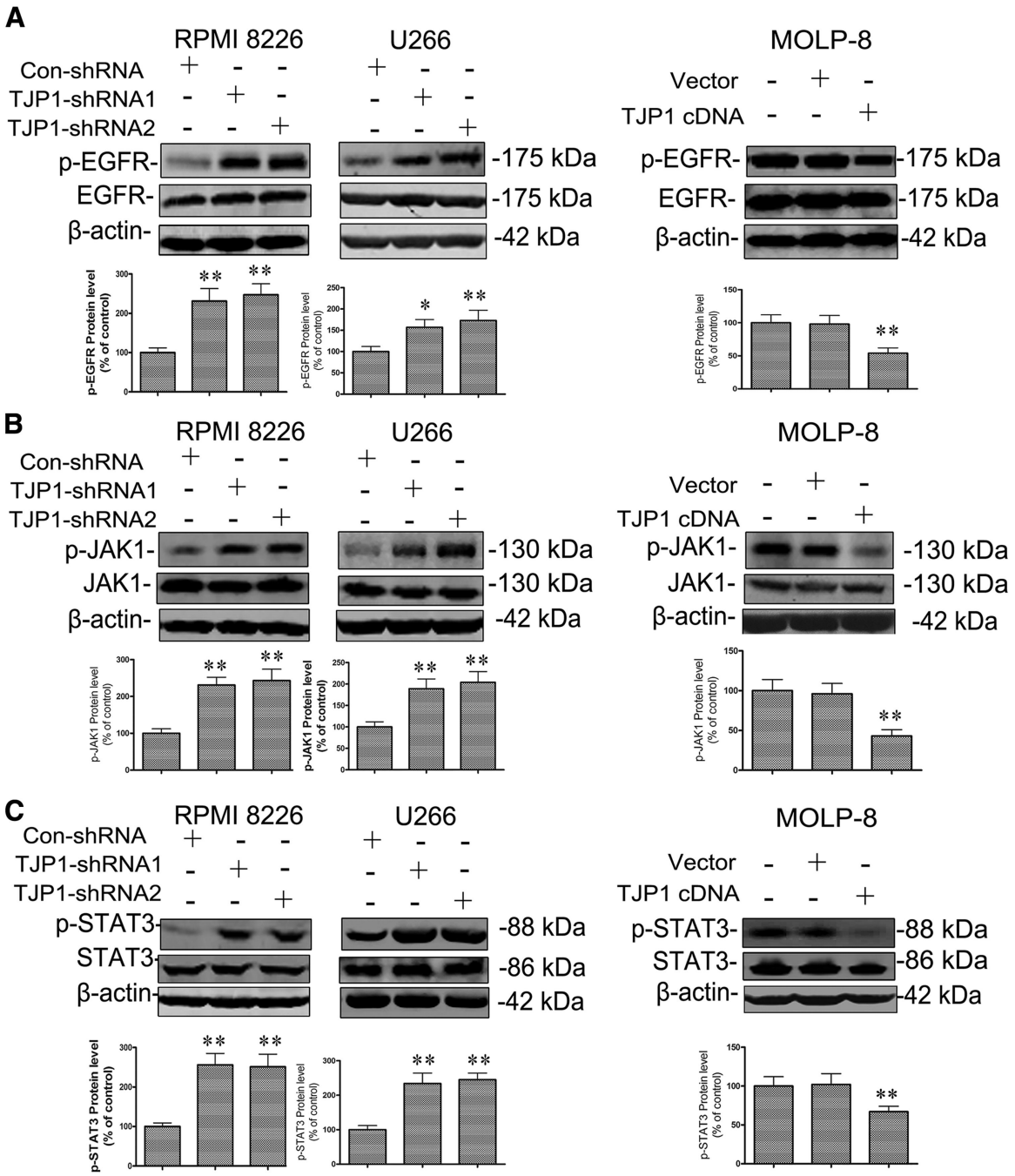

Figure 4. TJP1 and EGFR, JAK1 and STAT3 Activation Status

(A–C) RPMI 8226 (left) or U266 (middle) cells with TJP1 shRNAs or MOLP-8 cells overexpressing TJP1 (right) were analyzed for levels of phospho-EGFR (A), phospho-JAK1 (B), and phospho-STAT3 (C). Each membrane was reprobed for the corresponding total protein with a phosphorylation status-independent antibody and β-actin. Student's t test was performed on densitometry data from duplicate experiments to analyze significance. Error bars represent the mean ± SD. **$p < 0.05$, **$p < 0.01$ comparing TJP1 shRNA or cDNA cells with controls.

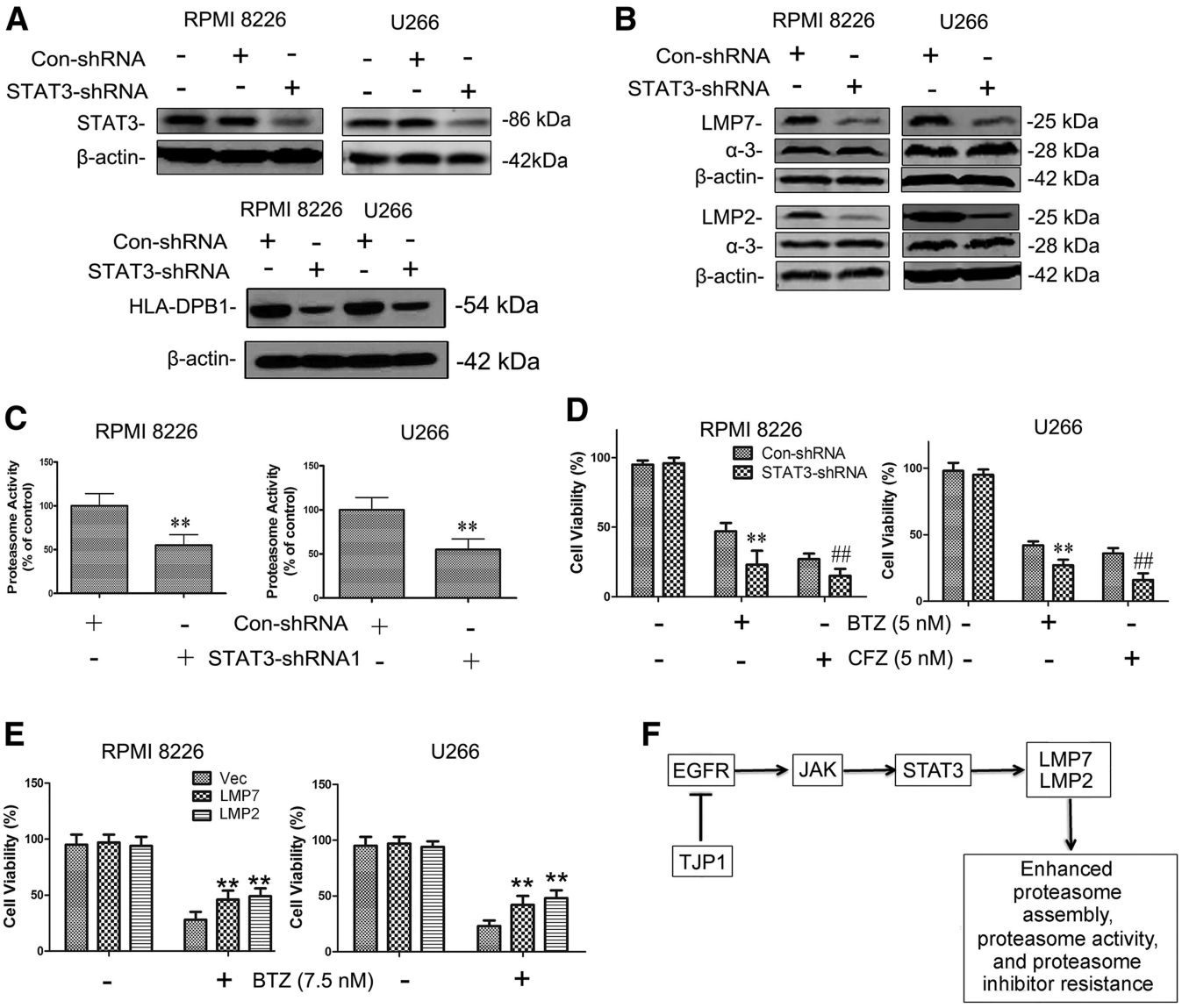

Figure 5. STAT3 and Proteasome Subunit Expression and Activity

(A and B) STAT3 and HLA-DPB1 protein levels (A), as well as LMP7 and LMP2 (B) determined by western blotting in RPMI 8226 (left) or U266 cells (right) with Con-shRNA, or a STAT3-shRNA.

(C) The ChT-L proteasome activity was determined in RPMI 8226 (left) or U266 cells (right) with Con-shRNA, or STAT3-shRNA. Error bars represent the mean ± SD. **p < 0.01 comparing STAT3-shRNA with Con-shRNA cells.

(D) Sensitivity to BTZ or CFZ of RPMI 8226 (left) or U266 cells (right) with a Con-shRNA, or STAT3-shRNA, was evaluated. Data from triplicate experiments are expressed as the mean ± SE in relation to the vehicle control cells arbitrarily set at 100%. Error bars represent the mean ± SD. **p < 0.01, ##p < 0.01 comparing STAT3-shRNA with Con-shRNA cells.

(E) RPMI 8226 (left) and U266 cells (right) transfected with Lentiviral controls (Vec) or vectors inducing LMP7 or LMP2 overexpression were treated with vehicle or BTZ for 72 hr. Their viability was determined, analyzed, and expressed as described above. Error bars

represent the mean ± SD. **p < 0.01 comparing viability in cells overexpressing LMP7 or LMP2 with vector controls.

(F) Our model suggests that EGFR activation results in downstream signaling through JAK1 and STAT3, and the latter induces LMP7 and LMP2 expression, which increases proteasome activity and PI resistance. In the presence of TJP1, EGFR/JAK/STAT activity is inhibited, which reduces proteasome capacity and sensitizes cells to PIs.

See also Table S4.

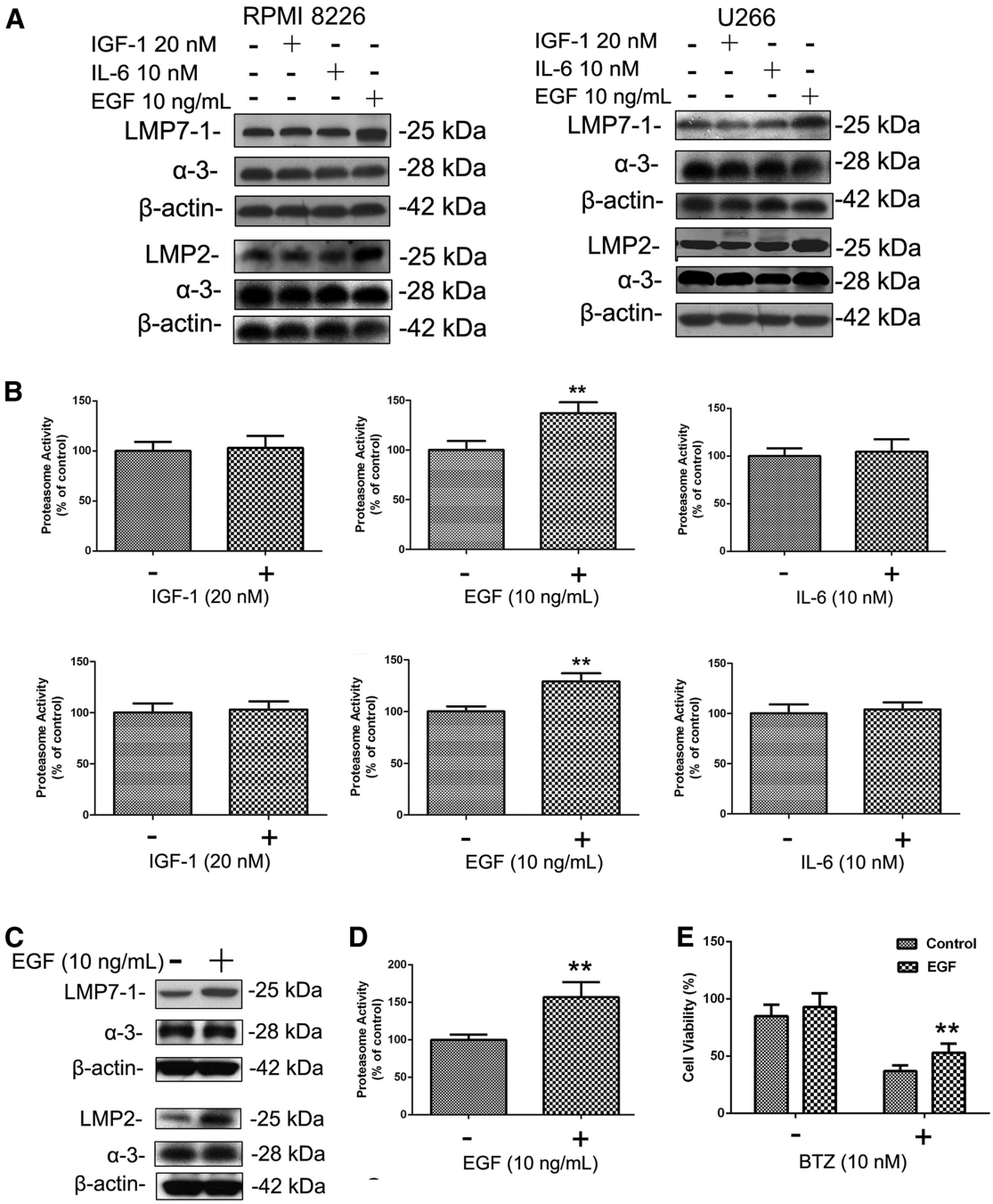

Figure 6. Cytokines and Proteasome Capacity

(A) RPMI 8226 (left) and U266 cells (right) were propagated in medium without serum, and then exposed to the indicated IGF-1, IL-6, and EGF concentrations for 48 hr. Cell extracts were then examined to determine the expression levels of LMP7, LMP2, β-actin, and α-3. (B) Proteasome ChT-L activity in RPMI 8226 (upper panels) or U266 cells (lower panels) propagated as above were determined. Error bars represent the mean ± SD. **p < 0.01 comparing ChT-L activity in EGF-treated cells with vehicle-treated cells.

(C) A549 cells were exposed to EGF or vehicle, and extracts were examined for their levels of LMP7, LMP2, α-3, or β-actin.

(D) ChT-L proteasome activity was determined in A549 cells exposed to EGF or vehicle as above. Error bars represent the mean ± SD. **p < 0.01 comparing ChT-L activity in EGF-treated cells compared with vehicle-treated cells.

(E) Viability was evaluated in A549 cells exposed to vehicle (−) or BTZ in the presence of vehicle or EGF at 10 ng/ml. Error bars represent the mean ± SD. **p < 0.05 comparing viability after BTZ treatment in EGF-exposed and vehicle-exposed cells.

See also Figure S2.

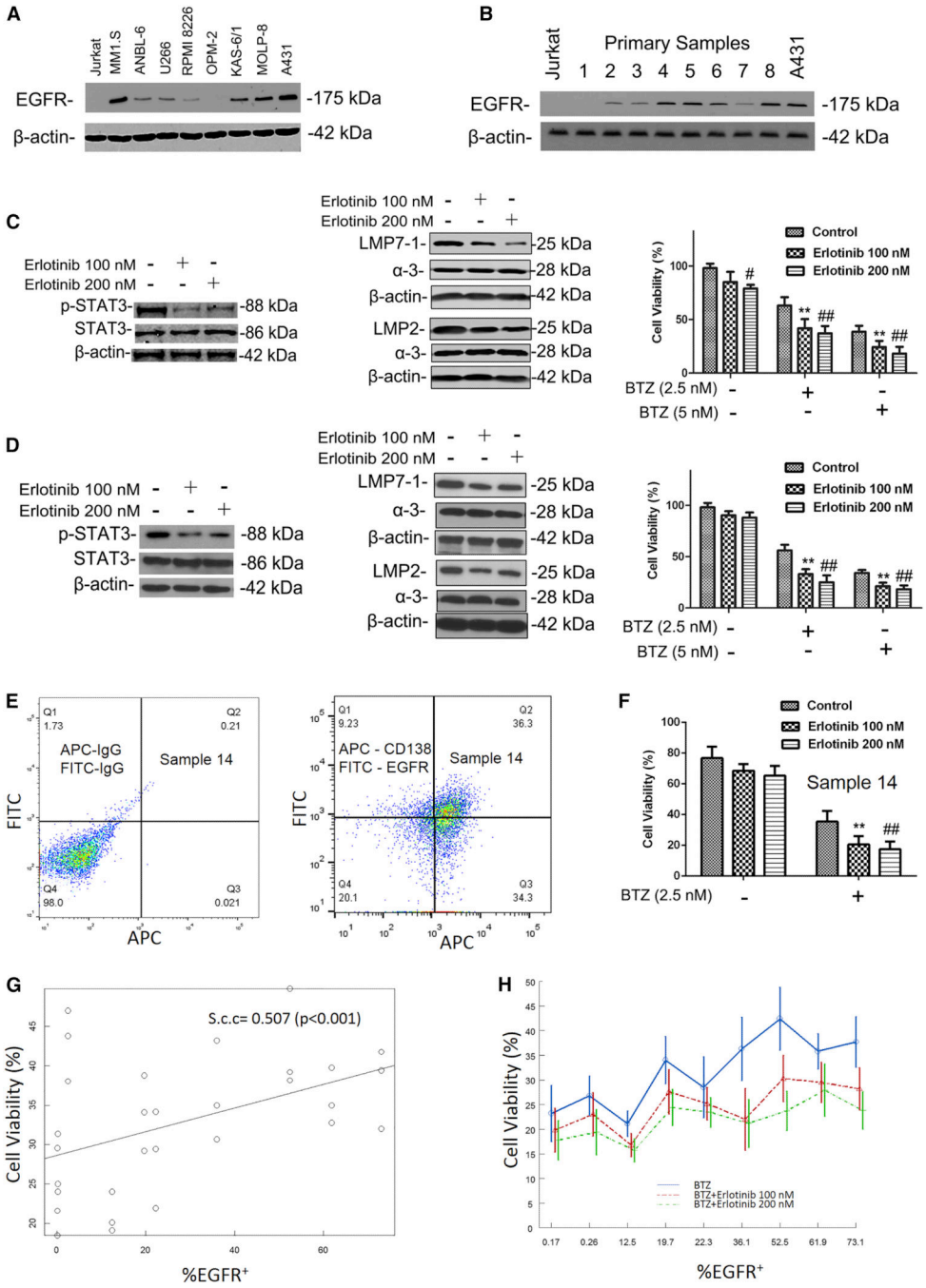

Figure 7. EGFR Expression and Targeting in Myeloma

(A and B) Extracts from MM1.S, ANBL-6, U266, RPMI 8226, OPM-2, KAS-6/1, and MOLP-8 myeloma cells, and from eight CD138^{+} primary myeloma patient samples (B) were examined for the expression of EGFR. Extracts of A431 human lung carcinoma cells were used as positive controls, and of Jurkat T cells as negative controls.

(C and D) RPMI 8226 (C) and U266 cells (D) were treated for 24 hr with erlotinib or vehicle, and extracts were subjected to western blotting to detect the activation status of STAT3 (left), and expression of LMP7 and LMP2 (middle). They were also exposed to BTZ

at the indicated concentrations, combined either with vehicle, or with erlotinib at 100 or 200 nM, and viability was measured. Error bars represent the mean ± SD. **p < 0.01 for the comparison of the combination of erlotinib at 100 nM and BTZ with the BTZ single-agent controls; #p < 0.05 for the same comparison with 200 nM erlotinib. ##p < 0.01 for the same comparison but with 200 nM erlotinib.

(E) Primary plasma cells from patient sample 14 were stained with non-specific APC-labeled immunoglobulin G (abscissa) and fluorescein isothiocyanate (FITC)-labeled antibodies (ordinate) as negative controls (left), or with allophycocyanin (APC)-labeled anti-CD138 and FITC-labeled anti-EGFR antibodies (right). Dot plots are shown of the resulting analyses obtained by flow cytometry.

(F) Plasma cells from (E) were exposed to vehicle or BTZ in the absence or presence of erlotinib, and viability was assessed. Error bars represent the mean ± SD. **p < 0.01, ##p < 0.01 for the two erlotinib concentrations compared with bortezomib alone.

(G) Cell viability in ten primary plasma cell isolates after bortezomib exposure is plotted as a function of their baseline EGFR expression.

(H) Mean cell viability, along with the SD, is plotted for the control primary samples with BTZ treatment only (blue curve), then after treatment with BTZ and either 100 nM (red) or 200 nM (green) erlotinib. Error bars represent the mean ± SD.

See also Figures S3–S7.

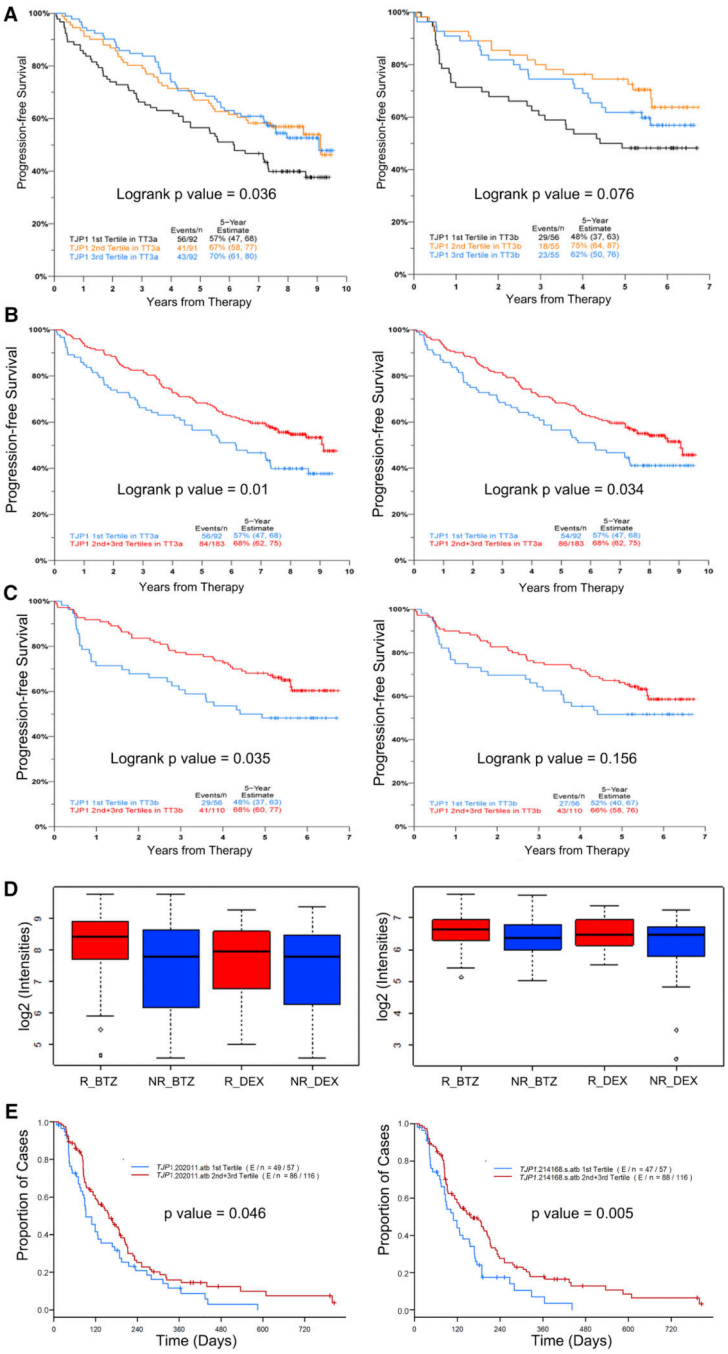

Figure 8. TJP1 Expression and Patient Outcomes

(A) PFS was evaluated in newly diagnosed myeloma patients treated with TT3a based on whether their TJP1 expression status was in the first (lowest expression) tertile (black curves), second (intermediate expression) tertile (yellow), or third (highest expression) tertile (blue). The log-rank test was used to determine significance, with data from TJP1 probe 202011_at represented on the left, and from probe 214168_s_at on the right throughout this figure.

(B and C) PFS for patients with TJP1 expression levels in tertile 1 (blue) and tertiles 2 and 3 (red) were determined from data for TT3a (B) and TT3b (C). Curves were plotted using Kaplan-Meier analyses, and significance was compared using the log-rank test.
(D) Comparisons were made between TJP1 expression and clinical outcomes for patients treated with BTZ. Single-agent BTZ data were from the combined gene-expression sets of the phase II and III trials in relapsed and/or refractory myeloma. Patients with a minor response or better (R; red box plots) were compared with all the other patients, who were classified as non-responders (NR; blue). In the box plot, the bottom and top indicate the first and third quartiles, respectively, the band in the box indicates the median, and the whiskers indicate the minimum and maximum values. The same analysis is also presented for patients treated with dexamethasone (DEX) from the control arm of the phase III bortezomib trial.
(E) TTP after bortezomib in the combined trial databases was analyzed using the Kaplan-Meier method based on whether patients had TJP1 expression in the second or third tertile (red), or the first tertile (blue).
See also Figure S8 and Tables S5–S8.